Compact Silicon Tunable Fabry–Pérot Resonator With Low Power Consumption

C. Angulo Barrios, V. R. Almeida, *Student Member, IEEE*, R. R. Panepucci, B. S. Schmidt, and M. Lipson, *Member, IEEE*

***Abstract*—We demonstrate a 20-μm-long tunable optical resonator integrated on a silicon-on-insulator waveguide. The microresonator consists of a planar Fabry–Pérot microcavity defined by deep Si/SiO_2 Bragg reflectors with a high finesse of 11.2. The device is electrically driven and shows a modulation depth as high as 53% for a power consumption of only 20 mW.**

***Index Terms*—Bragg reflector, Fabry–Pérot (F-P) cavity, integrated optics, optical modulator, silicon optoelectronics.**

I. Introduction

SILICON-BASED optical tunable (or active) devices, such as modulators, switches, and variable attenuators working at 1.3 and 1.55-μm fiber-optic communications-wavelengths are key components for the realization of Si CMOS optoelectronic circuits for applications such as fiber-to-home and local area networks [1]. Since crystalline Si does not exhibit linear electro-optic (Pockels) effect, Si active devices use either the thermooptic effect [2] or the free-carrier plasma dispersion effect to change the refractive index of Si and to produce a phase modulation. Typical changes of the refractive index due to these effects are small (on the order of 10^{-3}). Therefore, optical structures such as Mach–Zehnder interferometers [3], directional couplers [4], and low finesse Fabry–Pérott (F-P) cavities [2], [5], which transform the phase modulation into an intensity modulation, require long interaction lengths and high power consumption in order to achieve significant modulation depths. These long lengths and high powers are undesirable in order to achieve high levels of integration.

High finesse microcavities are very attractive for implementing active optical devices in a short length since the transmission close to their resonance wavelengths is highly sensitive to small index changes in the cavity [6]. In addition, since the refractive index variation may be achieved only in the microcavity region, the modulating power (for either heating or changing the free carrier concentration) required to produce the desired phase change can be made very small.

In this letter, we report on the fabrication and characterization of a 20-μm-long tunable F-P cavity on silicon-on-insulator (SOI). The F-P microcavity is defined on a rib waveguide by deep etched Si/SiO_2 distributed Bragg reflectors (DBRs). The use of deep DBRs increases significantly the reflectivity of the mirrors as compared with previous works [2], [5] and, therefore, the finesse of the cavity. The discussed structure is based on a p-i-n junction. As we showed theoretically in [6], such a configuration is expected to exhibit a very high modulation depth due to the electro-optic (plasma dispersion) effect. Here, we show experimentally that surface recombination induces a thermal modulation mechanism that dominates over the electro-optic effect. Most of the previously reported modulators based on the thermooptic effect are usually rather slow and/or require significant power consumption [2]. In this work, however, we demonstrate that due to the high finesse of the F-P cavity, significant modulation depth can be achieved using a drive power as low as 20 mW.

Manuscript received July 30, 2003; revised October 8, 2003. This work was supported by the National Science Foundation under Contract ECS-0 300 387 and the Defense Advanced Research Project Agency under Contract F49620-02-1-0396.

The authors are with the School of Electrical and Computer Engineering, Cornell University, Ithaca, NY 14853 USA (e-mail: cb265@cornell.edu).

Digital Object Identifier 10.1109/LPT.2003.822251

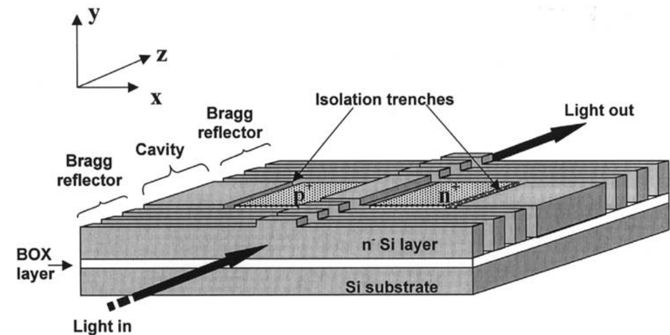

Fig. 1. Planar tunable F-P microcavity with deep Bragg reflectors and a p-i-n diode integrated on a single-mode SOI rib waveguide.

II. Device Structure and Fabrication

Fig. 1 shows a schematic of the device [6]. It was fabricatdon an SOI wafer with a 1.5-μm-thick undoped Si layer and a 1-μ m-thick buried oxide (BOX) layer. DBRs and isolation trenches were patterned by electron-beam (EB) lithography and etched by Cl_2 -based reactive ion etching (RIE) down to the BOX layer using SiO_2 as a mask. The DBR period and length of the trenches were $\sim$311 nm and $\sim$173 nm, respectively. SiO_2 was thermally grown to passivate the etched Si surfaces. The trenches were filled with SiO_2 by using low-pressure chemical vapor deposition. The rib waveguide was defined by photolithography and etched by CF_4-based RIE using photoresist as a mask. The height and width of the rib were $\sim$0.43 μm and $\sim$1 μm, respectively. SiO_2 was thermally grown for surface passivation of the rib sidewalls. Then, a 1-μm-thick SiO_2 cladding layer was deposited by plasma-enhanced chemical vapor deposition. Rectangular openings in the SiO_2 cladding layer were

1041-1135/04$20.00 © 2004 IEEE

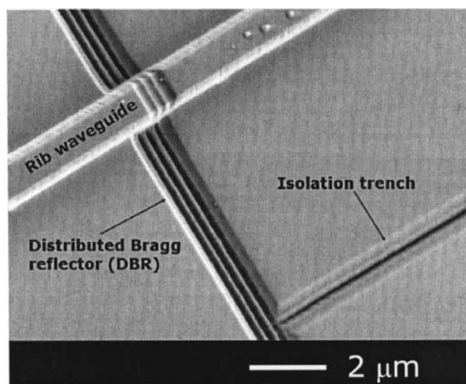

Fig. 2. Top view SEM photograph of a DBR and an isolation trench of the fabricated device.

made by EB lithography and CHF_3-based RIE for defining the doped regions shown in Fig. 1. Shallow n^+ and p^+ regions were created by ion implantation of As and BF_2, respectively. Ti and Al were deposited to form ohmic contacts and contact pads, respectively. Finally, the chip was cleaved, and the input and output facets were mechanically polished. Fig. 2 shows a scanning electron microscope (SEM) photograph of the planar F-P microcavity before doping.

III. Results and Discussion

Transmission experiments were performed by using a tunable laser (1520–1620 nm) as the input optical source. The probe beam was coupled directly into the rib waveguides by using a tapered-lensed fiber, collected by an output lens, and recorded by a photodetector. All the transmission experiments were made under transverse electric (TE) polarization. For the sake of normalization and waveguide loss evaluation, the transmitted power of a waveguide without any device was also measured.

Waveguide losses were evaluated by employing the F-P technique. Assuming a reflectivity of 0.3 at the Si/air interfaces, the measured losses in the rib waveguide for the TE-like polarized light were 22 dB/cm at $\sim$1.553 μm wavelength. We attribute this to scattering losses due to surface roughness of the rib sidewalls produced by the etching that, as indicated in [7], are significant for small rib widths. The coupling efficiency between the waveguide and the tapered-lensed fiber was measured to be around 8%. A theoretical coupling efficiency (integral overlap between the waveguide and fiber modes) of 20% was calculated by the beam propagation method (BPM). The discrepancy between the experimental and theoretical values may arise from facet polishing imperfections and fiber-waveguide alignment deviations. A fiber-to-waveguide tapered coupler similar to that reported in could be used to improve the coupling efficiency.

Fig. 3 (solid line) shows the transmission spectrum of the fabricated microcavity over the 1520–1600-nm wavelength range. The full width at half maximum (FWHM) of the resonance peak at $\lambda_p \sim 1.553$ μm is 1.54 nm. This represents a finesse, which is defined as the ratio between the full spectral range and the FWHM, of 11.2. A theoretical curve obtained by using a model described in [6] is also shown in Fig. 3 (dashed line). In

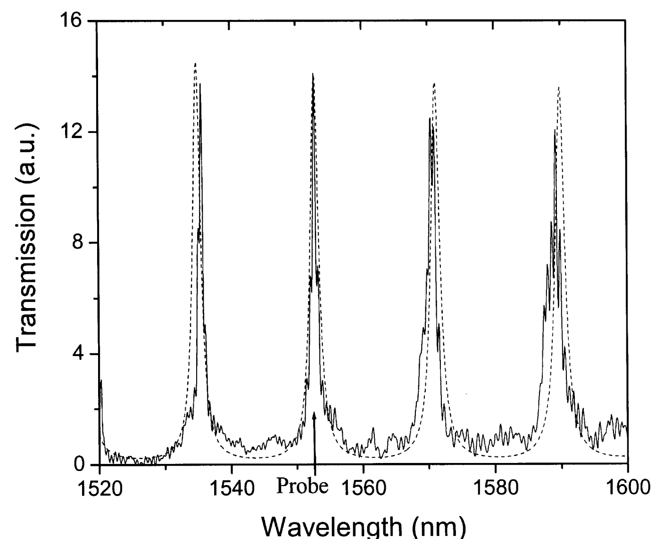

Fig. 3. Experimental (solid line) and calculated (dashed line) transmission spectra of the F-P microcavity for the fundamental TE-like mode in the 1520–1600-nm wavelength range.

this model, we include the experimental cavity internal loss of 0.04 dB [22 dB/cm (waveguide loss) $\times 18.12 \times 10^{-4}$ cm (cavity length)]. A fitting parameter that models the scattering losses in the DBRs was introduced. From comparison with the experimental spectrum, we estimate the scattering losses in the DBRs to be 7 dB. These are much higher than those in the waveguide due to the larger area of the etched surfaces that form the DBRs. One can see good fit around the considered resonance peak λ_p between the experimental and calculated curves. If the cavity internal losses are neglected and the DBRs are assumed to be scattering lossless, the theoretical analysis revealed FWHM and finesse values of 0.33 nm and 57.3, respectively.

The transient optical characteristics of the fabricated device were studied by applying an electrical pulse of 100 Hz and a 50% duty cycle. We measured rise and fall times of 1.05 and 1.19 ms, respectively, of the output optical power at $\lambda =$ 1552.89 nm and a drive current pulse (I) of 5.4 mA. A red-shift of the transmission spectrum of the biased device was also observed. This is a known signature of a thermooptic effect in Si (positive thermooptic coefficient [2]). We did not observe any effect on the output optical signal that could be attributed to dominating free carrier plasma dispersion. This may be due to the high sensitivity of the device to surface passivation [6]. High surface recombination may reduce significantly the total carrier lifetime, increasing the needed drive current to inject a significant amount of carriers. Thus, by increasing the current, the power dissipated in the series resistance of the p-i-n is increased, resulting in the heating of the cavity and leading to the strong thermooptic modulation effect. An improved surface passivation should enable modulation due to free-carrier dispersion effect [6]. The transient response exhibited by our device make it suitable to be used as a variable optical attenuator or as a modulator for low-frequency applications such as home and consumer appliances and remote environmental sensors.

Fig. 4 (squares) shows the measured modulation depth (M) of the device at a probe wavelength (λ_{pb}) of 1552.89 nm as a function of the dissipated power (P_d). M is defined as (P_{OFF} −

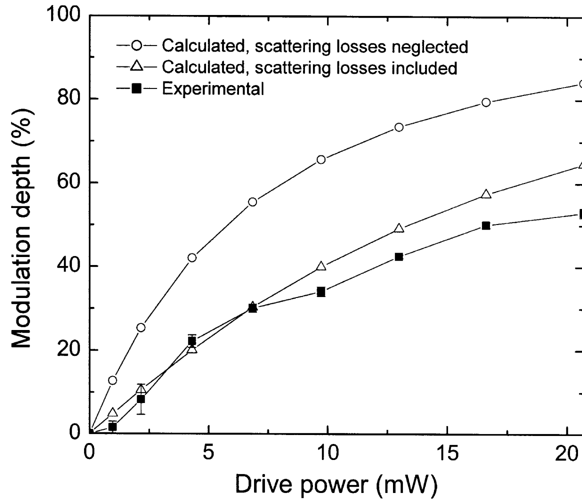

Fig. 4. Experimental (square dots) and calculated (triangular dots) modulation depth of the studied device at $\lambda_{\rm pb} = 1552.89$ nm as a function of the dissipated power. The calculated modulation depth of a similar device with negligible scattering losses is shown in circular dots.

$P_{\rm ON})/P_{\rm OFF}$, where $P_{\rm OFF}$ and $P_{\rm ON}$ are the transmitted optical powers in the OFF $(I = 0)$ and ON $(I \neq 0)$ states, respectively. A maximum modulation depth of 53% is obtained at $P_d = 20$ mW $(I = 5.4$ mA). This dissipated power is two orders of magnitude smaller than that reported for longer F-P cavity devices for a similar modulation depth [2], [5]. The small value of the power consumption should be attributed to the small size and high finesse of our F-P microcavity.

The dependence of the change in index with temperature $\Delta n_{\rm eff}/\Delta T$ provides an indication of the relative contributions of the free-carrier effect and the thermal effect to the modulation of the signal. This dependence can be estimated from a) the change in effective index as a function of the dissipated power and b) the temperature change for a given drive power. a) The change in effective index as a function of the dissipated power is obtained from the wavelength shift $(\Delta\lambda)$ for a given modulation depth (see Fig. 3). The change in effective index $(\Delta n_{\rm eff})$ is then given by $(\Delta n_{\rm eff}/n_{\rm eff}) = (\Delta\lambda/\lambda_{\rm pb})$, where $n_{\rm eff}$ (=3.3746) is the effective refractive index of the fundamental TE-like mode of the rib waveguide calculated by the BPM, and $\lambda_{\rm pb} = 1552.89$ nm. b) The temperature change (ΔT) for a given drive power is obtained by using a one-dimensional approximation, assuming that heat in the cavity is conducted to the surrounding Si through the isolation SiO_2 regions

$$\Delta T = R_{\rm th} P_d = \frac{P_d}{\frac{\kappa_{\rm SiO2} S_t}{2L_t} + \frac{\kappa_{\rm SiO2} S_{\rm BOX}}{L_{\rm BOX}} + \frac{\kappa_{\rm SiO2} S_{\rm DBR}}{2L_{\rm DBR}}} \quad (1)$$

where $R_{\rm th}$ is the equivalent thermal resistance of the SiO_2 regions, $\kappa_{\rm SiO2}$ is the thermal conductivity of SiO_2 (1.4 $\rm Wm^{-1}$ $\rm K^{-1}$), S_t is the area of the cavity surface in contact to a lateral isolation trench L_t is the length of a lateral trench, $S_{\rm BOX}$ is the area of the cavity in contact to the BOX layer, $L_{\rm BOX}$ is the thickness of the BOX layer, $S_{\rm DBR}$ is the area of the cavity surface in contact to a DBR, and $L_{\rm DBR}$ is the length of a DBR. Here, we assume that under dc conditions, the temperature is uniform through the whole cavity due to the high thermal conductivity of Si. From a) and b), we obtain a linear dependence of $\Delta n_{\rm eff}$ with ΔT with a slope of $+8.7 \times 10^{-5}$ $\rm K^{-1}$. This dependence is significantly smaller than the reported thermooptic coefficient of Si ($+1.86 \times 10^{-4}$ $\rm K^{-1}$ [2]) and may be due to the existence of free-carrier dispersion effect, which opposes the thermooptic effect.

In Fig. 4, we show the calculated modulation depth, using the estimated $\Delta n_{\rm eff}/\Delta T$, of the fabricated device (triangular dots) at $\lambda_{\rm pb} = 1552.89$ nm as a function of the dissipated power and considering the estimated scattering losses of 7 dB. The calculated modulation depth of a similar device with negligible scattering losses is also shown (circular dots). One can see that if the scattering losses in the device are lowered, the modulation depth is expected to increase to 80% for $P_d = 20$ mW. This modulation can be further increased using a top metal heater, as employed in conventional thermooptic devices [8], to avoid a competing plasma dispersion effect and decrease the dissipated power and the transient response of the device.

IV. Conclusion

We demonstrate a 20-μm-long electrically driven active planar F-P microcavity on Si. The microresonator, which is defined by high-aspect-ratio Si/SiO_2 DBRs, has a high finesse of 11.2. A p-i-n configuration is used to inject current into the cavity region. We show that the effective index of refraction in the cavity is modified due to a thermooptic effect. Due to the high finesse of the cavity, the device shows a modulation depth of 53% for a dissipated power of only 20 mW. If the scattering losses in the device are reduced, the modulation depth is expected to reach 80% for the same power dissipation. Micron size and low power consumption make this device very promising for use in Si-based integrated photonic systems on a chip (PSOC).

Acknowledgment

The device was fabricated at the Cornell NanoScience and Technology Facility (CNF).

References

[1] R. A. Soref, "Silicon-based optoelectronics," *Proc. IEEE*, vol. 81, pp. 1687–1706, Dec. 1993.
[2] G. Cocorullo, M. Iodice, and I. Rendina, "All-silicon Fabry–Pérot modulator based on the termo-optic effect," *Opt. Lett.*, vol. 19, no. 6, pp. 420–422, 1994.
[3] G. V. Treyz, P. G. May, and J.-M. Halbout, "Silicon Mach-Zehnder waveguide interferometers based on the plasma dispersion effect," *Appl. Phys. Lett.*, vol. 59, no. 7, p. 771, 1991.
[4] C. Z. Zhao, E. K. Liu, G. Z. Li, Y. Gao, and C. S. Guo, "Zero-gap directional coupler switch integrated into a silicon-on-insulator for 1.3-μm operation," *Opt. Lett.*, vol. 21, no. 20, p. 1664, 1996.
[5] C. Cocorullo, M. Iodice, I. Rendina, and P. M. Sarro, "Silicon thermooptical micro-modulator with 700 kHz −3 dB bandwidth," *IEEE Photon. Technol. Lett.*, vol. 7, pp. 363–365, Apr. 1995.
[6] C. A. Barrios, V. Almeida, and M. Lipson, "Low-power-consumption short-length and high-modulation-depth silicon electro-optic modulator," *J. Lightwave Technol.*, vol. 21, no. 4, pp. 1089–1098, 2003.
[7] A. G. Rickman, G. T. Reed, and F. Namavar, "Silicon-on-insulator optical rib waveguide loss and mode characteristics," *J. Lightwave Technol.*, vol. 12, pp. 1771–1776, Oct. 1994.
[8] R. L. Espinola, M.-C. Tsai, J. T. Yardley, and R. M. Osgood, "Fast and low-power thermooptic switch on thin silicon-on-insulator," *IEEE Photon. Technol. Lett.*, vol. 15, pp. 1366–1368, Oct. 2003.